DEVELOPMENT OF EMPIRICAL RELATIONSHIP TO PREDICT THE ADHESION STRENGTH OF HVOF SPRAYED WC-10NI-5CR COATINGS ON 35CrMo STEEL USING DESIGN OF EXPERIMENTS

Pradeep Raj Rajendran[1*], Thirumalaikumarasamy Duraisamy[2], Saravanan V[3], Ashokkumar Mohankumar[4]

Abstract

High-velocity oxy-fuel (HVOF) spray coating plays a major role in many surface treatment methods, which tend to improve erosion and corrosion resistance properties. HVOF is well known for its dense and high-quality coating ability. This is due to the less in-flight exposure time, which tends to have less oxide content because of its high-velocity properties. Among the number of process parameters, porosity and hardness are predominant factors while considering wear rate and corrosion behaviour analysis. The current study aims to optimise HVOF process parameters to obtain maximum adhesion strength values in the WC-10Ni-5Cr coating sprayed on 35 Mo Cr steel. The flow rates of oxygen, LPG, coating powder feed rate, and spray distance are selected in this study as these have a superior influence on the final condition of the coating. Statistical tools like the design of experiments (DoE), analysis of variants, and response surface methodology (RSM) were used to achieve the desired results. As per the result analysis, the oxygen flow rate has a higher effect on the adhesion value of the coating.

Keywords: High-velocity oxy-fuel spraying, adhesion strength, Response surface methodology

[1,2,4]*Department of Manufacturing Engineering, Annamalai University, Annamalai Nagar- 608002, Tamil Nadu, India.*
E: krsreeraj1@gmail.com
E: tkumarasamy412@gmail.com
E: ashokleadsaero12@gmail.com

[3]*Department of Mechanical Engineering, IRT Polytechnic College, Bargur, Tamilnadu, India*
E: saravananrubi@gmail.com

[1]Firstauthorandcorrespondingauthor
[2,3,4]Co authors

Introduction

Because they can resist wear and corrosion, WC-based cermet coatings are frequently used to shield materials from erosion and rust. It is widely assumed that high spray particle velocity and improved melting improve coating adhesion to a substrate.[1] The High Velocity Oxy-Fuel (HVOF) spray process has a high flame velocity of up to 2000 m/s. In comparison to conventional flame spraying and plasma spraying, such high velocity flames result in the formation of a high velocity spray particle stream. As a result, the HVOF spray process is a promising thermal spray process for depositing coatings with low porosity, resulting in higher density and bond strength.[2][3] Because of the high velocity associated with a relatively low flame temperature, the HVOF process is suitable for producing cermet coatings with a low porosity content (about 1%), which are denser and less oxidised than other thermal spray methods and cause no significant thermal and mechanical alterations to the substrate. The bond strength of HVOF coatings was not directly correlated with the conventional state parameters of spray particles such as temperature, velocity, and momentum.[4]

The bond strength of HVOF coatings is significantly influenced by the physical properties of the non-melting phases in a two-phase particle. Understanding different techniques for optimising and characterization of HVOF coatings necessitates a deeper understanding of the spray process, including starting materials, spray process, and particle-substrate interactions, in order to produce good coating quality with the appropriate properties and performance for specific applications.[5][6] The optimization of an HVOF spray process involving multiple factors and multiple responses, on the other hand, has not yet been reported in the literature. As a result, this study focuses on the use of response surface methodology (RSM) in developing empirical relationships to estimate the bond strength of WC-10 Ni 5 Cr coatings and optimising HVOF spray process parameters, including oxygen flow rate (O), LPG flow rate (L), standoff distance (S), and powder feed rate (F).

2. Experimental Procedure and methods.

Here, WC-10Ni-5Cr cermet powder (WOKA-3552, Oerlikon Metco) was selected as the coating material. From the scanning electron microscope (SEM), analysis of the purchased powder shows the particle size in the range of -45 to 15m (Fig. No. 1, a). The Electron Dispersive Spectrometer (EDS) confirms the chemical composition of the powder (Fig. No. 1, b). The substrate selected was commercially available 35CrMo Steel (ASTM A29/A29m) (AISI 4135), which is mainly used for the manufacturing of rolling mill gears, crankshafts, engine transmission parts, and large motor shafts. EDS confirms the chemical composition of the substrate (Fig. No. 1, c). Tables No. 1 and 2 shows the chemical composition of the substrate and coating powder.

WC-10Ni-5Cr powders are coated on 35CrMo substrate using HVOF Spraying facility found at Metallizing Equipment Co. Pvt. Ltd., Jodhpur, Rajasthan, India (Gun: HIPOSET-2700) with a coating thickness of 250 microns. Thickness of coating was observed with a micrometer (Digital) of 0.001mm accuracy (Mitutoyo, Japan). The substrate was preheated before coating by one whole torch cycle with a pass velocity of 0.8m/s at 120-180^0 C. 30 number of samples are prepared as per DOE(Table No.4) Acetone is used for ultrasonic cleaning of samples and grit blasted with corundum (320 ± 500µm) to increase the surface roughness. The normal surface roughness was observed as 6µm as per ASTM D7127-17 standards (Surface Roughness tester -Mitutoyo, Japan: Model Surf Test 301). Table No.3 shows the process factors of WC-10Ni-5Cr coatings. Fig No. 2 shows the coated substrate material.

Percent	C%	Si%	Mn%	P%	S%	Cr%	Mo%
comp	0.35	0.2	0.602	0.015	0.012	0.972	0.205

Table 1: Chemical composition of Substrate

Percent	C%	Cr%	Ni%	Fe%	W%
comp	5.4	5.03	10.25	0.06	Balance

Table 2: Chemical composition of coating powder

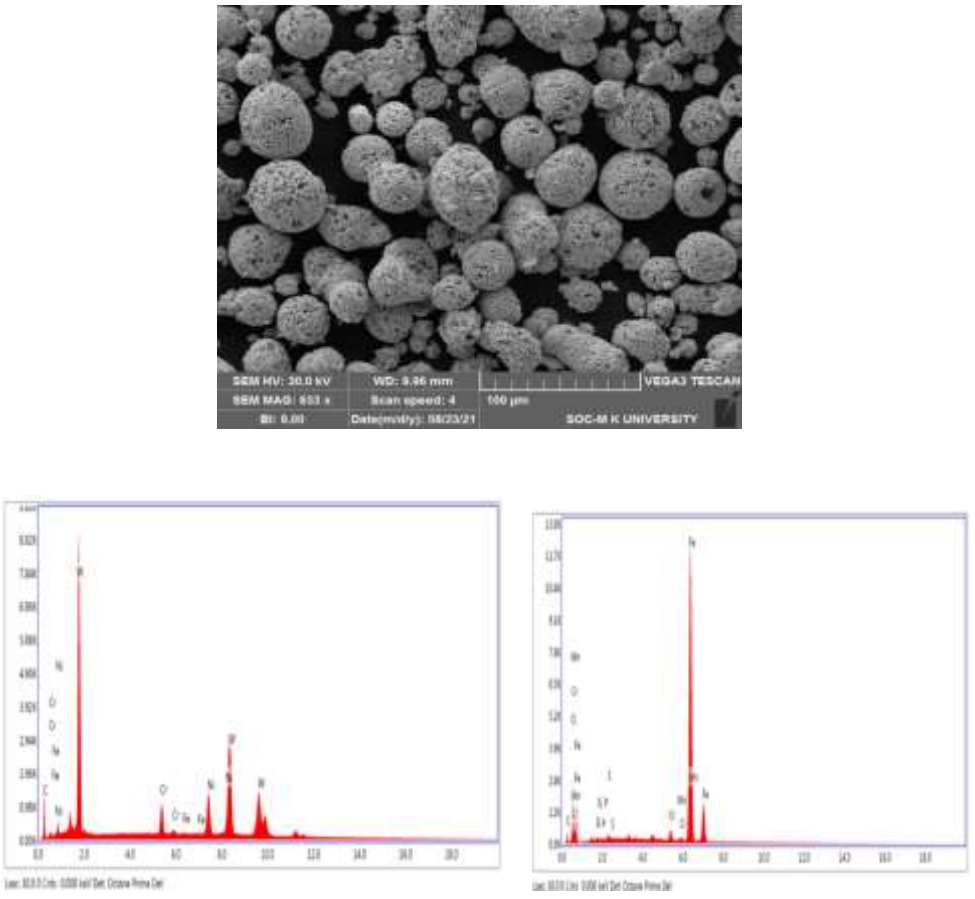

Figure1: SEM micrograph of (a) Received powder (b) EDS of received powder (c) EDS of base metal.

The act of HVOF coatings is significantly influenced by variables like fuel and gas flow rate, powder particle feed rate, and spray distance, according to published literature and laboratory experiments.[4} In order to attain high levels of adhesion values, it is crucial to control the ideal circumstances of the aforementioned parameters.[7] By HVOF spraying WC-10Ni-5Cr powders on 35CrMo Steel, enough tests were planned to determine the acceptable range of the aforementioned parameters by altering each individual factor separately. To prevent coating flaws including poor adherence to the base metal, uneven melting of powder particles, high porosity, and surface fissures, certain precautions are required.[8]

Fig. 2 shows the HVOF coated substrate with WC-10Ni-5Cr powder. Fig. No. 3 shows the SEM and EDS analysis of the coated material.

Using a universal testing equipment, the adhesive bond strength test was performed in accordance with ASTM C 633 standard (Make: FIE Blue Star, India; Model: UNITEK-94100). Three coated specimens were made and tested for each experimental condition in order to reduce experimental error. HTK ULTRA BOND-100 is a special purpose heat curable epoxy that is imported from HTK Hamburg, Germany and supplied by Metallizing Equipment Corporation (MEC PL), Jodhpur, India. At 190^0C for approximately 35-40 minutes with a load of 70 N/cm^2, glue is heated to cure. A few of the bond test specimens exhibit incomplete (mixed adhesive and cohesive) coating failures. The degree to which the remaining particles were covered after the bonding strength test, which measured the basic bond strength, was measured. Therefore, whenever a bond test revealed a partial failure, the coating area that remained on the substrate after the test, which was unbroken and did not detach or fail, was used to determine the true bond strength.

Here, RSM with CCD is used with the full replication method. The four main factors (F, O, S, L) were selected based on the previous literature results. Five different stages of the variables and values are shown in Table 3.

Fig. No. 2. Coated substrate

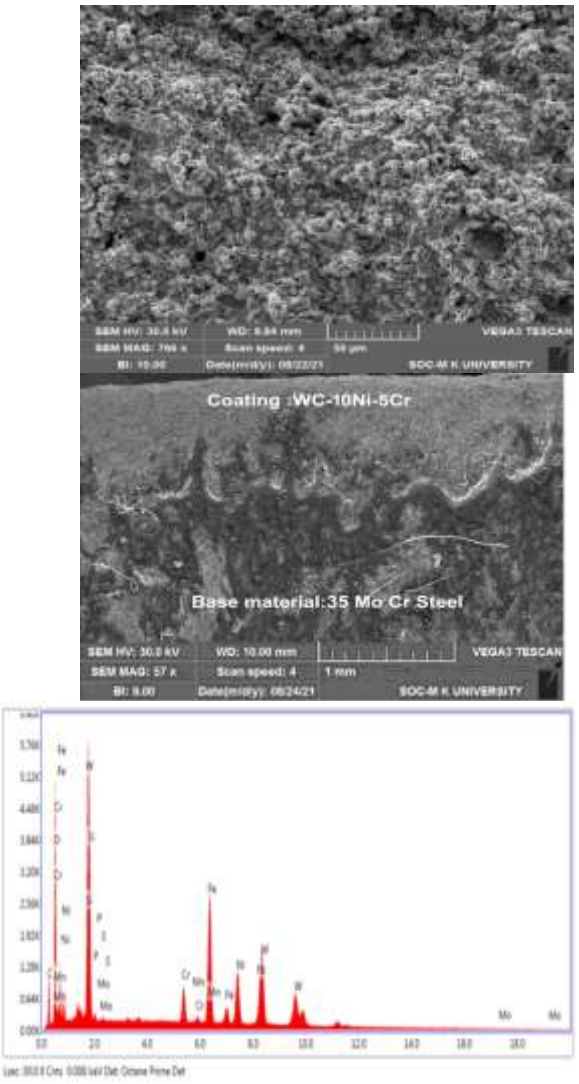

Figure 3: SEM micrograph of HVOF coated (a) top surface (b) Cross-section (c) EDS of cross-section.

S. No	Parameters	Notations	Units	Levels				
				-2	-1	0	1	2
1	Powder feed rate	F	gm/min	30	35	40	45	50
2	Oxygen flow rate	O	slpm	230	240	250	260	270
3	Spray Distance	S	Inch	6	6.5	7	7.5	8
4	LPG flow rate	L	slpm	45	50	55	60	65

Table 3: Parameters and possible working range of HVOF Coating

Sl. No	Coded value				Original value					Adhesion strength (MPa)
	F	O	S	L	F (gm/min)	O (slpm)	S (inch)	L (slpm)		
1	-1	-1	-1	-1	35	240	6.5	50		45
2	1	-1	-1	-1	45	240	6.5	50		47
3	-1	1	-1	-1	35	260	6.5	50		52
4	1	-1	-1	-1	45	260	6.5	50		43
5	-1	-1	1	-1	35	240	7.5	50		24
6	1	-1	1	-1	45	240	7.5	50		22
7	-1	1	1	-1	35	260	7.5	50		41
8	1	1	1	-1	45	260	7.5	50		43
9	-1	-1	-1	1	35	240	6.5	60		22
10	1	-1	-1	1	45	240	6.5	60		34
11	-1	1	-1	1	35	260	6.5	60		51
12	1	1	-1	1	45	260	6.5	60		47
13	-1	-1	1	1	35	240	7.5	60		25
14	1	-1	1	1	45	240	7.5	60		24
15	-1	1	1	1	35	260	7.5	60		23
16	1	1	1	1	45	260	7.5	60		57
17	-2	0	0	0	30	250	7	55		47
18	2	0	0	0	50	250	7	55		34
19	0	-2	0	0	40	230	7	55		22
20	0	2	0	0	40	270	7	55		48
21	0	0	-2	0	40	250	6	55		54
22	0	0	2	0	40	250	8	55		32
23	0	0	0	-2	40	250	7	45		20
24	0	0	0	2	40	250	7	65		44
25	0	0	0	0	40	250	7	55		45
26	0	0	0	0	40	250	7	55		47
27	0	0	0	0	40	250	7	55		44
28	0	0	0	0	40	250	7	55		48
29	0	0	0	0	40	250	7	55		45
30	0	0	0	0	40	250	7	55		46

Table 4: Experimental design matrix and result

Developing empirical relationships

RSM is used to relate the HVOF spray parameters and coating features. RSM is an exact and numerical tool that is usually used for DoE in order to develop mathematical models, optimize initial factors, and for obtaining a graphical model of results that help for clear analysis.

The following regression equation is used to signify the relationship between the variable and the responses. [9,10,11]

$$Y = B_0 + \sum B_I X_I + \sum B_{II} X_I^2 + B_{IJ} X_I X_J \quad -(1)$$

Where, Y and X_I, X_I^2, X_J are the predicted and variables in coded value; B_O B_I B_{II} B_I are constant, linear effect, squared effect, and interaction effect respectively.

Table 3 gives the reasonable limit of HVOF spray parameters. Here four variables are selected for analysis. So put K=4. Here 30 trials were performed as per the design shown in Table 4.

The adhesion strength of the HVOF sprayed coating are the depended variable of powder Particle feed rate (F), flow rate of oxygen (O), spray distance (S), flow rate of LPG(L).

Which conveyed as

$$\text{Response} = f(F, O, S, L) \quad -(2)$$

For the selected above factors, polynomial equation can be stated as

$$Y = b_o + b_1(F) + b_2(O) + b_3(S) + b_4(L) + b_{11}(FO) + b_{12}(FS) + b_{13}(FL) + b_{23}(OS) + b_{24}(OL) + b_{34}(SL) + b_{11}(F^2) + b_{22}(O^2) + b_{33}(S^2) + b_{44}(L^2) \quad -(3)$$

Where, b_o, b_1, b_2, b_3...b_{nn} are the middling responses and regression coefficients that hinge on on respective linear, interaction and squared terms of factors.

4. Results and discussion

'p' values and Student's 't-test are used to calculate the significance of respective coefficient in Tables

Here F, O, S, L, FO, FS, FL, OS, OL, SL, F2, O2, S2, L2 are taken as significant model terms. The values of "Prob>F' less than 0.5 displays that the model terms are important. The final empirical relationship was recognized with these significant coefficients.

AdhesionStrength=-
199.12500+8.15000(F)+8.14375(O)-
157.08333(S)-15.92083(L)-0.035000(FO)-
0.200000(FS)+0.070000(FL)+0.425000(OS)+0.077
500(OL)+1.55000(SL)-0.026250(F^2)-0.026563(O^2)-
2.62500(S^2)-0.153750(L^2) -(4)

The least probability value in Fisher's F-test gives a good regression model in order to calculate adhesion strength . The determination coefficient (R^2) is used to evaluate the goodness of fit. From the results, the R^2 values for the adhesion strength is 0.977. This shows that 97.77% of the investigational values are compatible with the desired results. An R^2 value close to 0.1 indicates a good statistical model for the analysis.

From the Fig. No. 4, the errors are normally distributed and also observed values matches with its experimental values healthy. (Correlation Graph).

To investigate the influencing tendency of the HVOF spray process parameters on the responses, 3D graphs were plotted under certain processing conditions. The 3D response surface and 2D contour plots are the graphical representations of the regression equations used to determine the optimum values of the variables within the ranges considered . Equation 4 (adhesion bond strength) is used to plot Fig5 (surface plots) and 6 (contour plots).

The increase in the levels of the elements under discussion causes the tensile bond strength to rise, reach an apex, and then fall, as shown in Fig. 5. The response plot's peak displays the strongest adhesion bond possible. The prediction of the responses for any zone of the experimental domain can be aided by these response contours. The multiple response optimization module in design-expert looks for a combination of factor levels that concurrently satisfies the demands (i.e., optimization criteria) set on each of the responses and process factors.

Here , the desired goals for each factor and response were chosen, and numerical and graphical optimization methods were applied.

Source	Sum of squares	df	Mean square	F-value	p-value	
Model	3061.77	14	218.70	32.39	<0.0001	Significant
F- powder feed rate	37.50	1	37.50	5.55	0.0324	
O- oxygen flow rate	1176.00	1	174.19	17.06	0.0001	
S-spray distance	640.67	1	640.67	94.89	0.0001	
L-LPG flow rate	22.04	1	22.04	3.26	0.0909	
FO	49.00	1	49.00	7.26	0.0167	
FS	4.00	1	4.00	0.5925	0.4534	
FL	49.00	1	49.00	7.26	0.0167	
OS	75.25	1	75.25	10.70	0.0052	
OL	240.25	1	240.25	35.59	0.0001	
SL	240.25	1	240.25	35.59	0.0001	
F^2	11.81	1	11.81	1.75	0.2057	
O^2	193.53	1	193.53	28.66	0.0001	
S^2	11.81	1	11.81	1.75	0.2057	
L^2	405.24	1	405.24	60.02	<0.0001	
Residual	101.27	15	6.67			
Lack of fit	90.44	10	9.044	4.7	0.0641	Not significant
Pure error	10.83	5	2.17		Cor total: corrected total	
Cor total	3163.04	29			PRESS: predicted error sum of squares	

Table 5: ANOVA values for the response Adhesion Strength

The objectives are intended to be combined into a general desirability function through the optimization process. A point or more are found through numerical optimization to maximise this function.[12] To designate regions where needs and proposed criteria are met simultaneously, one must superimpose or overlay critical response contours on a contour plot in the graphical optimization with multiple responses. Then, it is easy to visually seek for the ideal compromise. [13]

Numerical optimization should be done first when dealing with a large number of replies; otherwise, it may be impossible to discover a workable zone. The region of realistic response values in the factor space is shown by the graphical optimization.[14] Shaded areas are those that do not meet the optimization criterion. A criterion was used in the numerical optimization portion. The goal is to increase the tensile and lap shear bond strengths. The lower and/or upper bounds for each response's graphical optimization have been selected based on the outcomes of the numerical optimization. The graphical optimization adopted the same criterion that was put out in the numerical optimization.

Contour plots play a very important role in the study of a response surface.[15,16] The contour plots are illustrated in Fig. 6 Each contour curve represents an infinite number of combinations of values of two test factors derived from the second-order quadratic equation within the considered range. The maximum predicted value is identified by the

surface confined in the smallest ellipse or circle of the contour diagram.

The elliptical contour map implies that the interactions between the respective elements are substantial, whereas the circular contour plot suggests that they are insignificant. Additionally, a contour map is created to visually illustrate the region of the ideal factor settings. Such a plot can be more intricate for second-order response surfaces as opposed to the straightforward parallel series that can appear with first-order empirical relationships. Characterizing the response surface close to the stationary point is typically required once it has been located.

Characterization involves identifying whether the stationary point found is a minimum response or maximum response or a saddle point. To classify this, it is more straightforward to examine it through a contour plot.

The above-mentioned response values could be achieved using the following optimized parameter settings: oxygen flow rate: 247 slpm, LPG flow rate: 54 slpm, standoff distance: 6 inch and powder feed rate: 48 gpm. The above values (factor values and response values) were also verified using the graphical optimization. The graphical optimization result allows visual inspection to choose the optimum coating condition. The shaded areas of the overlay plot are the regions that do not meet the proposed criteria.

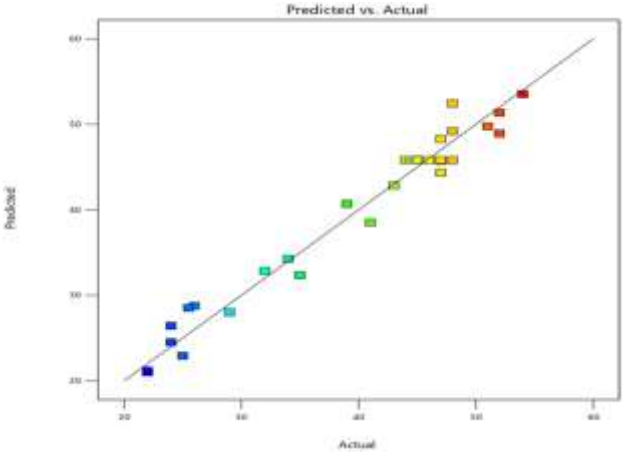

Fig. No. 4: The Correlation Graph for adhesion strength

HVOF spray Parameters				Adhesion Strength (By Experiment)	Adhesion strength (By modal)	variation %
Powder feed rate (gm/min)	Oxygen flow rate (slpm)	Spray distance (inch)	LPG flow rate (slpm)			
38	242	6	52	48	47	-3.82
40	260	6.5	62	52	51.3	-2.46
42	265	7	58	46	47.4	4.41
44	270	8	65	40	40.77	-2.71

Table 6: Authentication of results for optimization procedure

Fig. 7 shows the graphical optimization plot. Three more confirmation tests were carried out to corroborate the model's accuracy, comparing the outcomes to what would be expected under ideal circumstances. Table 6 presents the results of the mean experimental response. The anticipated values and the validated response values exhibit good agreement.

The abrupt acceleration that occurs when a sufficiently molten particle strikes the substrate leads to a build-up of pressure at the particle-substrate interface; the high pressure inside the particle causes the melted material to flow laterally or the ductile solid material to deform. From the point of impact, the liquid spreads outward and makes a splat. Spreading is halted as a result of viscous deformation and surface energy's work on the particle's kinetic energy. The droplets' velocity, size, molten state, chemistry, and angle of collision with the surface all affect how splats develop. It is also dependent on the substrate's temperature, reactivity, and surface topography.[16-24]

This procedure establishes the coating's macroscopic and microstructural properties. When combined with optimal particle velocity, optimum particle temperature leads to a reduction in the

material's dynamic viscosity and a higher degree of flattening. Additionally, a higher degree of flattening results in a thinner splat and a larger area of the splat surface in contact with the underlying material, which increases deposition efficiency and results in materials with better bond strengths.

Due to the proper in-flight temperature in the case of the coating created under ideal spray conditions, the majority of the particles undergo melting, making it easier for each splat to cover the surface topography onto which it flattens. The highest amount of bonding strength that can be achieved is seen in WC-10Ni-5Cr cermet coatings that have been sprayed under ideal conditions. The attainable bonding strength was found to be poor under less than ideal circumstances.

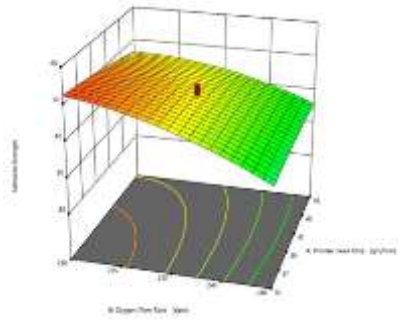

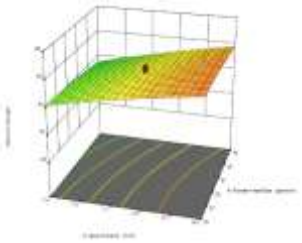

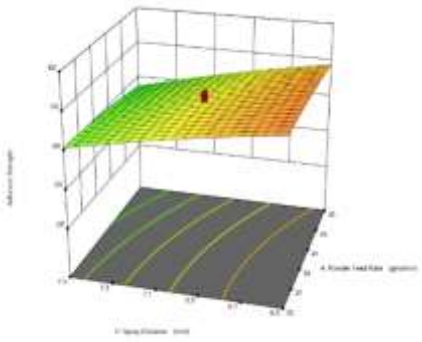

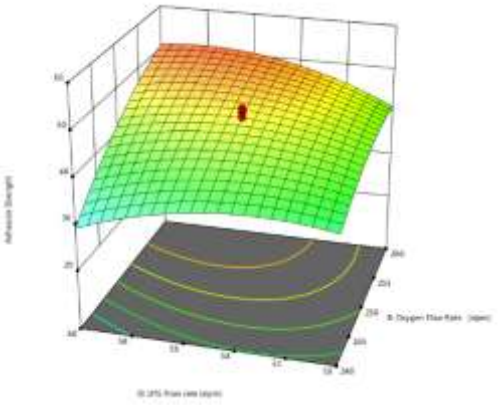

Fig. No. 5. Response graph for effect of parameters on adhesion strength (a) F and O (b) F and S (c) F and L (d) O and S (e) O and L (f) S and L

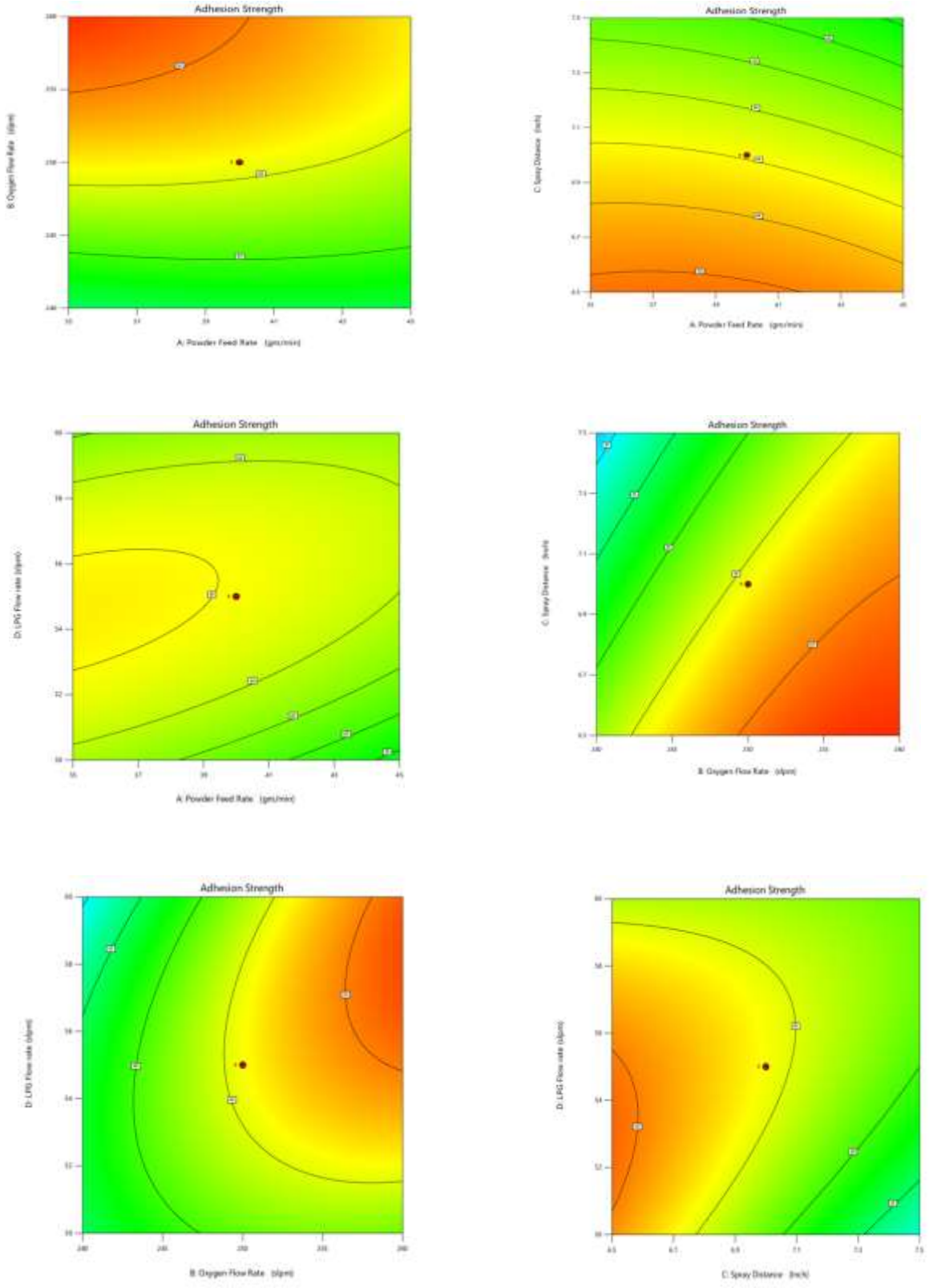

Fig. 6 Contour plots for adhesion strength. (a) Effect of O and F, (b) Effect of S and F, (c) Effect of L and F, (d) Effect of S and O (e) Effect of L and O (f) Effect of L and S.

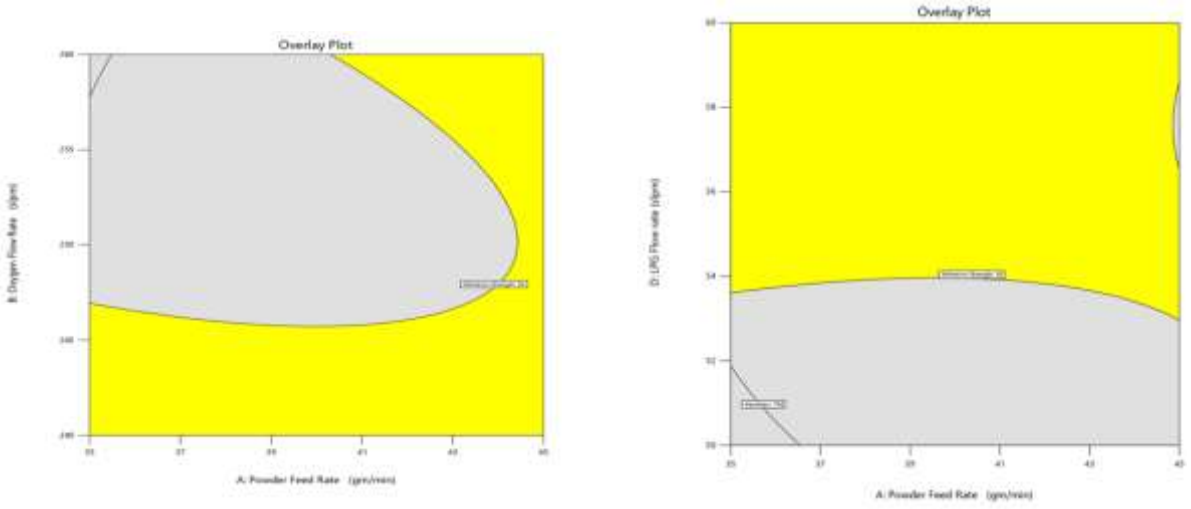

Fig. No. 7. Overlay plots of optimized HVOF coating parameters to achieve maximum adhesion strength

Validation of Optimization Procedures

The HVOF spray process parameters that were recommended by the numerical modelling (suggested solutions) were used in the confirmation experiments, with the oxygen flow rate, LPG flow rate, powder feed rate and spray distance remaining at 247 lpm, 54 lpm, 48 gpm, and 6 inch, respectively. Between the projected values and experimental values, a small difference was discovered (Table 7). The parameters and observed results from two more sets of experiments that were carried out above and below the optimised HVOF spray technique are shown in Table 7.

Based on these findings, it was deduced that changing the HVOF spray process parameters from the ideal conditions caused the powder particles to melt too quickly or too slowly due to differences in the air-to-fuel ratio, burn too long or too short due to differences in spray distance, and deposit too much or too little powder on the substrate due to too much or too little carrier gas flow, which reduced adhesion[25].

Table 7: Authentication of results for optimization procedure

Expt. No	HVOF spray Parameters				Adhesion strength (Mpa)
	Powder feed rate (gm/min)	Oxygen flow rate (slpm)	Spray distance (inch)	LPG flow rate (slpm)	
1	48	247	6	54	52.5
2	45	244	5.5	51	46
3	51	250	6.5	57	42

Conclusions

1. Empirical relationships were developed to estimate the adhesion bond strength and lap shear bond strength of HVOF-sprayed WC-CrC-Ni coatings incorporating HVOF spray operational parameters.
2. From ANOVA test results (as per ‘‘F’’ value), it is found that the oxygen flow rate has greater influence on adhesion strength and LPG flow rate has least influence on adhesion strength of the coatings.
3. The optimum deposition parameters yielded maximum adhesion bond strength and lap shear bond strength of HVOF-sprayed WC-CrC-Ni coatings are oxygen flow rate: 247 lpm, LPG flow rate: 54 lpm, standoff distance: 6 inch and powder feed rate: 48 gpm.

Acknowledgments

The authors wish to express their sincere gratitude to department of manufacturing engineering, Annamalai University, Tamil Nadu, India for providing the facilities for the research work. Also the authors wish to express deepest gratitude to Metallizing Equipment Co. Pvt. Ltd., Jodhpur, Rajasthan, India and The Government College of Engineering, Burgur, Tamil Nadu, India for Providing the Facilities for coating and testing.

References

1. Vaßen, R., Bakan, E., Gatzen, C., Kim, S., Mack, D.E., Guillon, O., 2019. Environmental Barrier Coatings Made by Different Thermal Spray Technologies. Coatings, 9 , 784.
2. Shrikant Josh., 2019. Per Nylen. Advanced Coatings by Thermal Spray Processes: A review. Technologies, 7, 79.
3. Romanov D., Moskovskii, S., Konovalov, S., Sosnin, K., Gromov, V., Ivanov, Y., 2019. Improvement of copper alloy properties in electro-explosive spraying of ZnO-Ag coatings resistant to electrical erosion. Journal of Materials Research and Technology, 8, 6, pp. 5515-5523.
4. Pradeep Raj, Rajendran., Thirumalaikumarasamy, Duraisamy., Ramachandran Chidambaram Seshadri., Ashokkumar, Mohankumar., Sathiyamoorthy, Ranganathan., Guruprasad, Balachandran., Kaliyamoorthy, Murugan., and Laxmi, Renjith, 2022. Optimisation of HVOF Spray Process Parameters to Achieve Minimum Porosity and Maximum Hardness in WC-10Ni-5Cr Coatings" *Coatings* 12, no. 3: 339.
5. Mohankumar., Ashokkumar., Thirumalaikumarasamy Duraisamy., Ramachandran Chidambaramseshadri., Thirumal Pattabi., Sathiyamoorthy Ranganathan, Murugan Kaliyamoorthy, Guruprasad Balachandran., Deepak Sampathkumar., and Pradeep Raj Rajendran., 2022. Enhancing the Corrosion Resistance of Low Pressure Cold Sprayed Metal Matrix Composite Coatings on AZ31B Mg Alloy through Friction Stir Processing. Coatings, 12, 135.
6. Kannan, Mathivanan., Thirumalaikumarasamy Duraisamy., Thirumal Pattabi., and Ashokkumar Mohankumar., 2021. Investigate the corrosion properties of stellite coated on AZ91D alloy by plasma spray technique. Thermal Science, 209-209.
7. Ashokkumar, M., Thirumalaikumarasamy, D., Thirumal, P., & Barathiraja, R., 2021. Influences of Mechanical, Corrosion, erosion and tribological performance of cold sprayed Coatings A review. Materials Today: Proceedings, 46, 7581-7587.
8. Mathanbabu, M., Thirumalaikumarasamy, D., Thirumal, P., & Ashokkumar, M., 2021. Study on thermal, mechanical, microstructural

properties and failure analyses of lanthanum zirconate based thermal barrier coatings: A review. Materials Today: Proceedings, 46, 7948-7954.

9. Giovanni, Straffelini., Matteo, Federici., 2020. HVOF Cermet Coatings to Improve Sliding Wear Resistance in Engineering Systems: A review. Coatings, 10, 886.
10. Brezinová, J., Guzanová, A., Tkáčová, J., Brezina, J., Ľachová, K., Draganovská, D., Pastorek, F., Maruschak, P., Prentkovskis, O., 2020. High Velocity Oxygen Liquid-Fuel (HVOLF) Spraying of WC-Based Coatings for Transport Industrial Applications. *Metals*, *10* , 1675.
11. Tilger, M., Biermann, D., Abdulgader, M., Tillmann, W., 2019. The Effect of Machined Surface Conditioning on the Coating Interface of High Velocity Oxygen Fuel (HVOF) Sprayed Coating. *J. Manuf. Mater. Process*, *3*, 79.
12. Wu, M., Pan, L., Duan, H., Wan, C., Yang, T., Gao, M., Yu, S., 2021. Study on Wear Resistance and Corrosion Resistance of HVOF Surface Coating Refabricate for Hydraulic Support Column. Coatings, 11 , 1457.
13. M.A. Javed., A.S.M. Ang., C.M. Bhadra., R. Piola., W.C. Neil., C.C. Berndt., M. Leigh., H. Howse., S.A. Wade., 2021. Corrosion and mechanical performance of HVOF WC-based coatings with alloyed nickel binder for use in marine hydraulic applications. Surface & Coatings Technology, 418.
14. S.Vignesh., K .Shanmugam., V.Balasubranian., K.Sridhar., 2017. Identifying the optimal HVOF spray parameters to attain minimum porosity and maximum hardness in iron based amorphous metallic coatings .Defence technology ,doi:10.1016/j.dt.2017.03.001.
15. Karthikeyan., V. Balasubramanian., R. Rajendran., 2014. Developing empirical relationships to estimate porosity and microhardness of plasma-sprayed YSZ coatings Ceramic International, 40, 3171–3183.
16. Vignesh, S., Balasubramanian, V., Sridhar, K., Thirumalaikumarasamy, D., 2019. Slurry Erosion Behavior of HVOF-Sprayed Amorphous Coating on Stainless Steel. Metallography, Microstructure, and Analysis, doi:10.1007/s13632-019-00552-1.
17. Prasad, R.V., Rajesh, R., Thirumalaikumarasamy, D., 2021. et al. Sensitivity analysis and optimisation of HVOF process inputs to reduce porosity and maximise hardness of WC-10Co-4Cr coatings. Sādhanā 46, 149.
18. Ribu, D. C., Rajesh, R., Thirumalaikumarasamy, D., & Vignesh, S., 2021. Influence of rotational speed, angle of impingement, concentration of slurry and exposure time on erosion performance of HVOF sprayed cermet coatings on 35CrMo steel. Materials Today: Proceedings, 46, 7518–7530.
19. Thirumalvalavan., Subramanian., & Senthilkumar., Natarajan., 2019. Experimental investigation and optimization of HVOF spray parameters on wear resistance behaviour of Ti 6Al 4V alloy. Comptes Rendus de l'Academie Bulgare des Sciences, 72(5), 664-673.
20. Qiao, Lei., Wu, Yuping., Hong, Sheng., Long, Weiyang., Cheng, Jie., 2020. Wet abrasive wear behavior of WC-based cermet coatings prepared by HVOF spraying. Ceramics International,

S027288422032705X–. doi:10.1016/j.ceramint.2020.09.009.

21. K. Murugan., A. Ragupathy., V. Balasubramanian., K. Sridhar., 2014. Optimization of HVOF spray parameters to attain minimum porosity and maximum hardness in WC-10 Ni-4 Cr coatings. Surface and Coatings Technology 247 , 90-102.
22. Thermsuk, Somkiat., Surin, Prayoon., 2019. Optimization Parameters of WC-12Co HVOF Sprayed Coatings on SUS 400 Stainless Steel. Procedia Manufacturing, 30 , 506–513.
23. Baumann, Ingor., Hagen, Leif., Tillmann, Wolfgang., Hollingsworth, Peter., Stangier, Dominic., Schmidtmann, Gunnar., Tolan, Metin., Paulus, Michael., Sternemann, Christian., 2020. Process characteristics, particle behavior and coating properties during HVOF spraying of conventional, fine and nanostructured WC-12Co powders. Surface and Coatings Technology, 126716– . doi:10.1016/j.surfcoat.2020.126716.
24. Liu, S., Wu, H., Xie, S., Planche, M.-P., Rivolet, D., Moliere, M., & Liao, H., 2021. Novel liquid fuel HVOF torches fueled with ethanol: relationships between in-flight particle characteristics and properties of WC-10Co-4Cr coatings. Surface and Coatings Technology, 408, 126805. doi:10.1016/j.surfcoat.2020.126805.
25. Guzanová, A., Brezinová, J., Draganovská, D., Maruschak, P.O., 2019. Properties of coatings created by HVOF technology using micro- and nano-sized powder, Koroze a Ochrana Materialu, 63 (2), pp. 86-93, doi: 10.2478/kom-2019-0011.